Relative influences of atmospheric chemistry and transport on Arctic ozone trends

M. P. Chipperfield* **& R. L. Jones†**

** The Environment Centre, University of Leeds, Leeds LS2 9JT, UK*
† Department of Chemistry, University of Cambridge, Lensfield Road, Cambridge CB2 1EW, UK

The reduction in the amount of ozone in the atmospheric column over the Arctic region, observed during the 1990s[1,2], resembles the onset of the Antarctic ozone 'hole' in the mid-1980s, but the two polar regions differ significantly with respect to the relative contributions of chemistry and atmospheric dynamics to the ozone abundance. In the strong, cold Antarctic vortex, rapid springtime chemical ozone loss occurs throughout a large region of the lower stratosphere, whereas in the Arctic, although chemical ozone depletion has been observed[3–11], the vortex is generally much smaller, weaker and more variable[12]. Here we report a model-based analysis of the relative importance of dynamics and chemistry in causing the Arctic ozone trend in the 1990s, using a state-of-the-art three-dimensional stratospheric chemistry–transport model. North of 63° N we find that, on average, dynamical variations dominate the interannual variability, with little evidence for a trend towards more wintertime chemical depletion. However, increases in the burden of atmospheric halogens since the early 1970s are responsible for a large (14%) reduction in the average March column ozone, but this effect is mostly caused by increased destruction throughout the year rather than by halogen chemistry associated with wintertime polar statospheric clouds. Any influence of climate change on future average Arctic ozone amounts may thus be dominated by possible circulation changes, rather than by changes in chemical loss.

Early observations of stratospheric ozone indicated the important role of transport, as well as chemistry, in determining the distribution of stratospheric ozone[13]. Recent studies have indicated that changes in atmospheric circulation may have contributed to observed changes in mid-latitude ozone from 1979 to 1991[14,15]. Three-dimensional (3D) chemistry–transport models (CTMs) are now able to represent the seasonal chemistry and transport of stratospheric trace species. These models[16–18] specify meteorological analyses for the winds and temperatures, allowing the calculated distribution of atmospheric trace species to be compared directly with measurements. We have now updated our 3D CTM to be suitable for multiannual integrations[19], an advance which allows us to model the interannual variability in stratospheric dynamics and chemistry in a single simulation. We integrated the CTM using a horizontal resolution of 7.5° × 7.5°, and 12 potential-temperature levels from 335 K to 2,700 K (resolution of ~3 km in the lower stratosphere). The start of the simulation was October 1991 using horizontal winds and temperatures from the UK Meteorological Office[20]. The CTM calculates the vertical (diabatic) motion from a radiation scheme. The standard CTM includes a description of heterogeneous chemistry occurring on liquid/solid polar stratospheric clouds (PSCs) and mid-latitude sulphate aerosols[19]. The standard CTM simulations used a constant halogen loading of 3.6 parts per billion by volume (p.p.b.v.) of total chlorine and 20 parts per trillion (10^{12}) by volume (p.p.t.v.) of total bromine.

Newman *et al.*[1] reported satellite data which show that the March monthly-mean ozone-column values in the region 63–90° N (March $\langle O_3 \rangle_{63-90}$) decreased from values near 470 dobson units (DU) in the early 1970s to values as low as 355 DU in 1997. They chose to analyse this region as it typically contains the polar vortex, which is often decaying by this time. We note, however, that the size of the vortex in March is very variable and, even with a conservative (large) definition of the vortex extent, this diagnostic will include mid-latitude air. For example, the size of the polar vortex was around 50% of this area in March 1992 and 80% in March 1997 (although the large vortex was not zonally symmetric). Figure 1a shows the monthly $\langle O_3 \rangle_{63-90}$ observations of Newman *et al.*[1] for the Arctic (March) and Antarctic (October) from 1990 extended to the end of 1998. The Antarctic $\langle O_3 \rangle_{63-90}$ values are small and show little interannual variability. This is a result of the large chemical removal of ozone within the large, stable Antarctic polar vortex which occurs

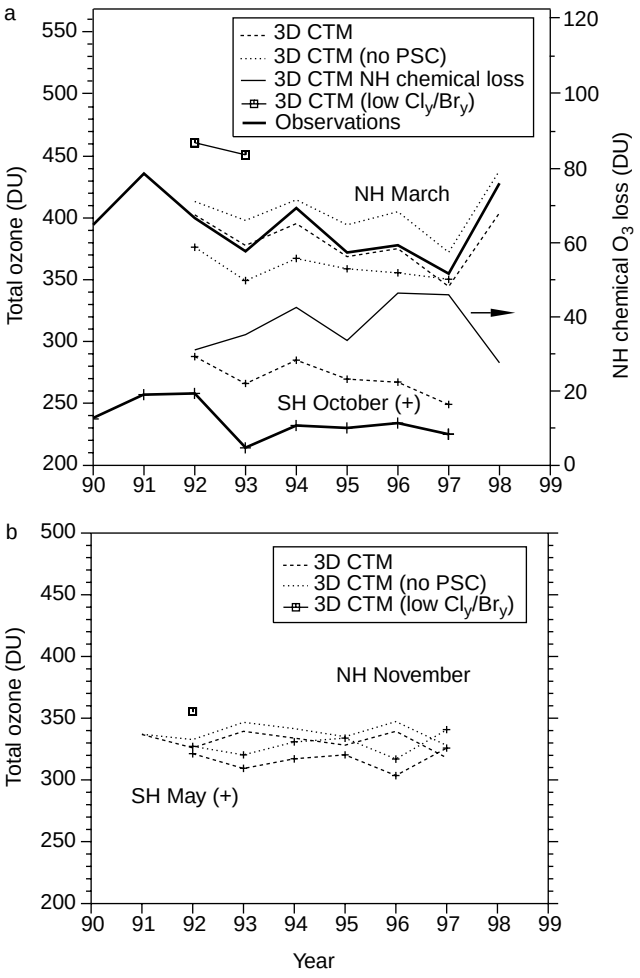

Figure 1 Monthly average column ozone (DU) between 63° and 90° latitude. **a**, March in the Northern Hemisphere (NH) and October in the Southern Hemisphere (SH); **b**, November in the NH and May in the SH. Panel **a** also shows the satellite observations of Newman *et al.*[1] extended until March 1999. Results are shown from three 3D model simulations. The standard model (dashed line) uses present-day halogen loadings and includes the effects of heterogeneous chemistry on polar stratospheric clouds (PSCs). The model includes a time-dependent distribution of liquid aerosols which is taken from 2D model calculations. The dotted line shows results of the simulation without the effects of chlorine activation on liquid and solid PSCs and aerosols. The squares show the NH results of the model simulation with lower halogen loadings (1.35 p.p.b.v. chlorine; 10 p.p.t.v. bromine). Panel **a** (right-hand axis) also shows the seasonal NH chemical ozone depletion diagnosed directly from the standard model run. For all model simulations, the mixing ratio of O_3 in the troposphere (below ~12 km) was assumed to be 50 p.p.b.v. in the NH and 40 p.p.b.v. in the SH.

regularly every year. In contrast, the Arctic March $\langle O_3 \rangle_{63-90}$ values are generally much larger and show more interannual variability. In particular, the lowest March value in 1997 of around 355 DU was followed by a much larger value in 1998 of around 428 DU. In fact, the modelled $\langle O_3 \rangle_{63-90}$ in March 1997 indicates only a net 5 DU increase since November 1996.

The standard 3D CTM integration captures well the observed interannual variability in $\langle O_3 \rangle_{63-90}$ in the Arctic region, to within ~20 DU. The CTM reproduces all of the relative minima and maxima and, in particular, the strong minimum in 1997, followed by the large increase in 1998. (The CTM also reproduces synoptic-scale features which determine the time evolution of column ozone at specific sites related to the motion of the polar vortex[19].) Given the excellent agreement, we have diagnosed the relative roles of chemistry and transport within the model. We have quantified the modelled rapid winter/spring chemical O_3 loss by two methods. First, we used a passive O_3 tracer to diagnose the total chemical loss each winter. On 15 December of each year this tracer was initialized with the model O_3 field. Second, we repeated the model experiment without heterogeneous reactions on solid PSCs or direct chlorine-activating reactions on cold liquid aerosols. The first method gives a direct quantification of the chemical O_3 loss in each winter; the second method illustrates the effect of polar processing in all seasons throughout the integration. Over the latitude range 63–90° N, the average column chemical loss is around 30–40 DU (~50% larger than the difference between the two 3D model experiments as the different ozone fields feed back into the transport via calculated descent rates). This mean chemical loss reflects the relatively small area of the Arctic polar vortex relative to the area poleward of 63° N (the maximum local mean model column loss in March 1997 is around 80 DU, similar to other calculations for the mid-March loss of that year[21]) and that distortions to the polar vortex can cause O_3-depleted vortex air to extend equatorward of 63° N. When presented as this monthly average over the area 43–90° N, which includes air both inside and outside the vortex, the modelled interannual variability in the rapid vortex ozone depletion in March is relatively small, although the cold winters of 1995/96 and 1996/97 do show the largest chemical loss. While we acknowledge that the model simulation (run at low resolution) may underestimate the magnitude of the observed chemical loss—as shown in the Antarctic comparison in Fig. 1a and indicated by other model studies[11,22]—the interannual variability in the vortex chemical loss is much less than the overall observed and modelled variability in column O_3 north of 63° N.

Figure 1b shows the $\langle O_3 \rangle_{63-90}$ from the model simulations at the start of the winters (November in the Northern Hemisphere, NH; May in the Southern Hemisphere, SH). The model predicts similar mean ozone values in the two polar regions, with only small interannual variation (for example, a standard deviation (s.d.) of 8 DU in the NH). This is supported by our analysis of Nimbus 7 TOMS data for November and May averaged over the sunlit area of the polar regions (H. Teyssèdre, personal communication). This

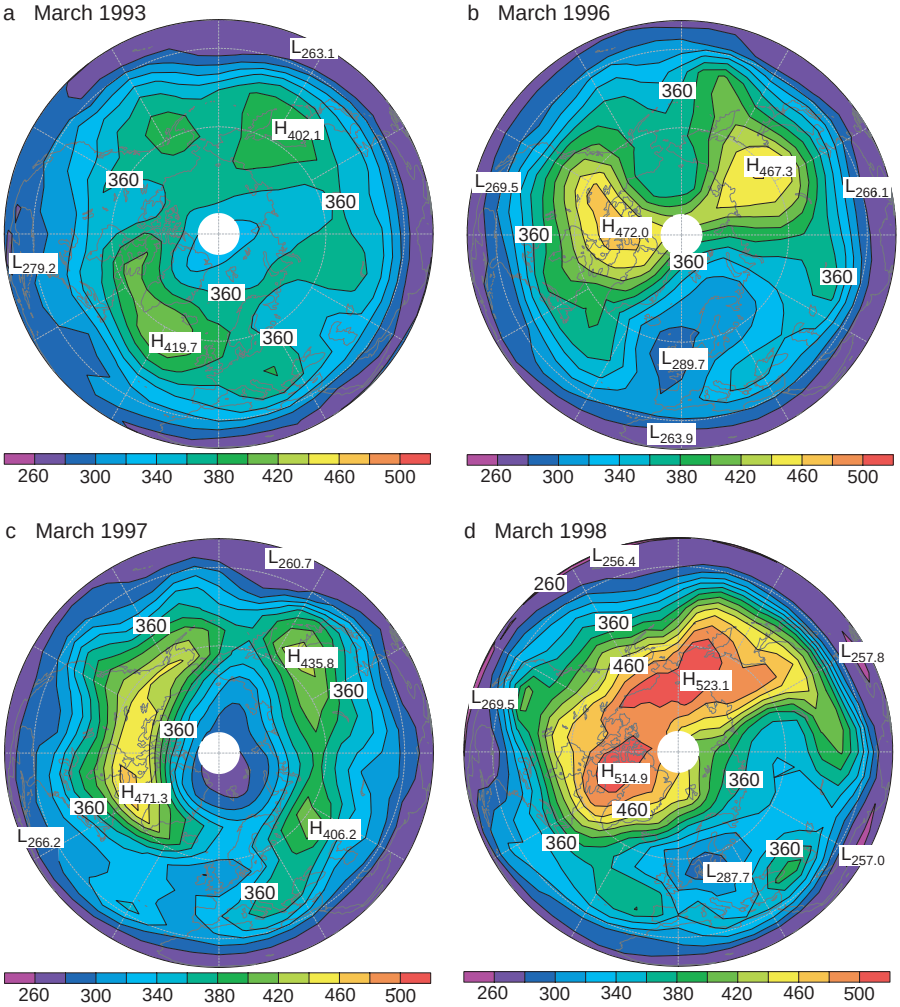

Figure 2 Northern Hemisphere March average column ozone (DU). Results are from the standard model run for 1993 (**a**), 1996 (**b**), 1997 (**c**) and 1998 (**d**). Contour interval is 20 DU. The symbols H and L indicate relative maxima and minima, respectively.

suggests that all NH winters start with similar values of $\langle O_3 \rangle_{63-90}$ and that the interannual differences observed in March are determined by transport (and to a lesser degree, chemistry) during the winter. Comparison of Fig. 1a and b emphasizes that over the winter the SH experiences a strong net reduction due to the domination of chemical loss, while the NH experiences a strong increase due to transport which is partly offset by chemical loss. Having already diagnosed the chemical loss, and having shown that the modelled November means are similar from year to year, we can argue that the interannual differences in March are due to differences in the wintertime transport, which affect the size and stability of the vortex. Descent, and transport of ozone, is weakest when the vortex is strong and undisturbed, which are also the conditions that lead to cold temperatures. In contrast, a warm, disturbed vortex will result in stronger diabatic descent, and a larger increase in ozone. Further comparison of Fig. 1a and b shows that the dynamical build-up of O_3 during winter 1997/98 was particularly strong. The Arctic mean O_3 column for November 1997 was slightly lower than other years but the March 1998 column was much larger. Long-lived model tracers (such as total inorganic chlorine) indicate that the modelled wintertime high-latitude descent was indeed strongest in 1997/98 (not shown).

Figure 2 shows the March monthly mean O_3 for selected winters from the standard model run. The values of $\langle O_3 \rangle_{63-90}$ generally combine low column values associated with the mean position of the polar vortex and much higher values in the extra-vortex region (see, for example, the 1990s data of Figure 2 in ref. 1). In 1998 the modelled values in this larger extra-vortex region were much higher than previous model years.

The meteorological analyses used to force the CTM are only available from October 1991, so we cannot study directly the observed ozone variation throughout the 1970s and 1980s. However, we have investigated the effect of the increased atmospheric halogen loading by repeating the first 2 years of the standard model run with reduced halogen loadings typical of the early 1970s[23] (Cl_y, 1.35 p.p.b.v.; Br_y, 10 p.p.t.v.). This reduced halogen loading yields Arctic $\langle O_3 \rangle_{63-90}$ values which are higher by 8% in November and 14% in March. This March difference is similar in magnitude to the reduction observed by Newman *et al.*[1] between the early 1970s and early 1990s. Comparing Figs 3 and 2a shows that under the low-halogen conditions the calculated March ozone column is larger throughout the polar region; not just in the region of the polar vortex, but also throughout the 'collar' region. These model results suggest that, although interannual differences in wintertime halogen-catalysed ozone loss is a minor contributor to the observed $\langle O_3 \rangle_{63-90}$ variation in the 1990s (that is, the s.d. of chemical loss is 8 DU compared to an s.d. of the March $\langle O_3 \rangle_{63-90}$ of 21 DU), the increase in halogens has nevertheless caused a reduction in Arctic $\langle O_3 \rangle_{63-90}$. This loss is due to increased destruction throughout the stratosphere throughout the year, which is not related to PSCs. Figure 4 shows differences in the November and March zonal-mean ozone fields. The increased halogens have caused a reduction of around 1 p.p.m.v. (up to 20%) in the upper stratosphere, and smaller mixing-ratio reductions—which will contribute to the column decrease—throughout the lower stratosphere which are not linked to polar processes. Diagnosis of the model shows that the main catalytic cycles responsible for this decrease involve $ClO^{\cdot} + O^{\cdot}$ in the upper stratosphere, and cycles involving $ClO^{\cdot} + BrO^{\cdot}$ or $HO_2^{\cdot}$ in the lower stratosphere, with $ClO^{\cdot} + ClO^{\cdot}$ important in the polar lower stratosphere.

Overall, our multiannual 3D model simulations have quantified many features of the observed interannual variations in Arctic ozone. Although PSC-related halogen chemistry certainly destroys O_3 within the polar vortex, the model shows that the mean springtime abundance of ozone in the entire polar region (north of 63° N) is mainly controlled by dynamics acting over the winter (the mean dynamical increase in $\langle O_3 \rangle_{63-90}$ from November to March in our 7-year simulation was 80 DU, partially offset by a mean chemical loss of 38 DU). This dynamical build-up shows strong interannual variability which controls the observed interannual variability in the mean column ozone. Over this large area, the signal of rapid halogen-catalysed loss inside the vortex (which can be as small as

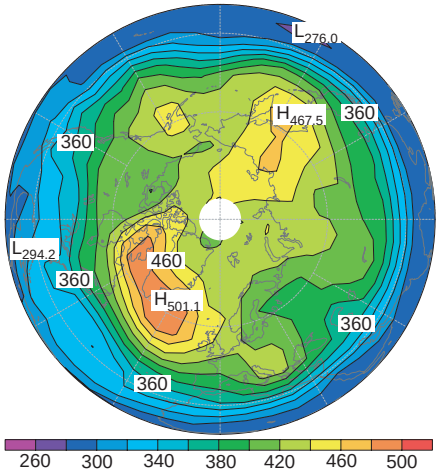

Figure 3 Northern Hemisphere average column ozone (DU) for March 1993. Results are from the model run with low halogen loading. Contour interval is 20 DU. The symbols H and L indicate relative maxima and minima, respectively.

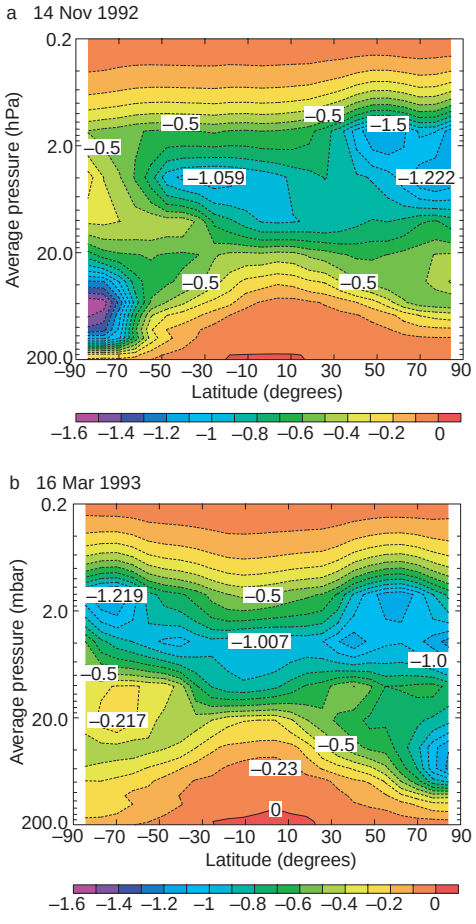

Figure 4 Difference in zonal mean O_3 mixing ratio (p.p.m.v.). Shown is the difference between the low-halogen experiment and the standard model run. **a**, 14 November; **b**, 16 March.

50% of this area in March) is reduced. However, the increases in stratospheric halogen loading due to anthropogenic emissions has contributed significantly to the springtime decrease since the 1970s. The observed decadal decrease in column O_3 values in March north of 63° N may contain a large (>50%) contribution from slow, year-round, halogen-catalysed depletion.

These results have implications for future levels of ozone in the Arctic region. Although the amount of PSC-induced chemical depletion within the vortex may be enhanced due to stratospheric cooling[24], the main factor determining the average ozone column to date in a given winter is dynamics. This transport is affected by interannual variability, but may also be subject to a trend—for example, due to stratospheric O_3 decrease or other climate-related effects. Possible future circulation changes (for example, those that make the Arctic vortex more Antarctic-like) could significantly change mean wintertime ozone levels by transport alone. Also, while Shindell *et al.*[24] pointed out the potential feedback between stratospheric cooling which may delay the recovery of Arctic ozone as halogen levels decrease, the contribution of halogens to the decadal decrease in ozone in the larger extra-vortex region may be expected to follow the halogen loading more closely, unless cooling extends PSC activation outside the vortex. □

Received 26 October 1998; accepted 11 June 1999.

1. Newman, P. A. *et al.* Anomalously low ozone over the Arctic. *Geophys. Res. Lett.* **24,** 2689–2692 (1997).
2. Fioletov, V. E. *et al.* Long-term ozone decline over the Canadian Arctic to early 1997 from ground-based and balloon observations. *Geophys. Res. Lett.* **24,** 2705–2708 (1997).
3. Rex, M. *et al.* Prolonged stratospheric ozone loss in the 1995–96 Arctic winter. *Nature* **389,** 835–838 (1997).
4. Müller, R. *et al.* Chlorine activation and ozone depletion in the Arctic vortex: Observations by the Halogen Occultation Experiment on the Upper Atmosphere Research Satellite. *J. Geophys. Res.* **101,** 12531–12554 (1996).
5. Müller, R. *et al.* Severe chemical ozone loss in the Arctic during the winter 1995–96. *Nature* **389,** 709–712 (1997).
6. Müller, R. *et al.* HALOE observations of the vertical structure of chemical ozone depletion in the Arctic vortex during winter and early spring 1996–1997. *Geophys. Res. Lett.* **24,** 2717–2720 (1997).
7. Manney, G. L. *et al.* Arctic ozone depletion observed by UARS MLS during the 1994–95 winter. *Geophys. Res. Lett.* **23,** 85–88 (1996).
8. Manney, G. L., Santee, M. L., Froidevaux, L., Waters, J. W. & Zurek, R. W. Polar vortex conditions during the 1995–96 Arctic winter: Meteorology and MLS ozone. *Geophys. Res. Lett.* **23,** 3203–3206 (1996).
9. Manney, G. L., Froidevaux, L., Santee, M. L., Zurek, R. W. & Waters, J. W. MLS observations of Arctic ozone loss in 1996–97. *Geophys. Res. Lett.* **24,** 2697–2700 (1997).
10. Sinnhuber, B. M., Langer, S., Klein, U., Raffalski, U. & Kunzi, K. Ground based millimeter-wave observations of Arctic ozone depletion during winter and spring of 1996/97. *Geophys. Res. Lett.* **25,** 3327–3330 (1997).
11. Hansen, G., Svenøe, T., Chipperfield, M. P., Dahlback, A. & Hoppe, U. P. Evidence of substantial ozone depletion in winter 1995/96 over northern Norway. *Geophys. Res. Lett.* **24,** 799–802 (1997).
12. Zurek, R. W., Manney, G. L., Miller, A. J., Gelman, M. E. & Nagatani, R. M. Interannual variability of the north polar vortex in the lower stratosphere during the UARS mission. *Geophys. Res. Lett.* **23,** 289–292 (1996).
13. Dobson, G. M. B. Observations of the amount of ozone in the earth's atmosphere and its relation to other geophysical conditions. *Proc. R. Soc. Lond. A* **129,** 411–433 (1930).
14. Hood, L. L., McCormack, J. P. & Labitzke, K. An investigation of dynamical contributions to midlatitude ozone trends in winter. *J. Geophys. Res.* **102,** 13079–13093 (1997).
15. Steinbrecht, W., Claude, H., Kohler, U. & Hoinka, K. P. Correlations between tropopause height and total ozone: Implications for long-term changes. *J. Geophys. Res.* **103,** 19183–19192 (1998).
16. Rood, R. B., Allen, D. J., Baker, W. E., Lamich, D. J. & Kaye, J. A. The use of assimilated stratospheric data in constituent transport calculations. *J. Atmos. Sci.* **46,** 687–701 (1989).
17. Lefèvre, F., Brasseur, G. P., Folkins, I., Smith, A. K. & Simon, P. Chemistry of the 1991–1992 stratospheric winter: Three-dimensional model simulations. *J. Geophys. Res.* **99,** 8183–8195 (1994).
18. Chipperfield, M. P. *et al.* Analysis of UARS data in the southern polar vortex in September 1992 using a chemical transport model. *J. Geophys. Res.* **101,** 18861–18881 (1996).
19. Chipperfield, M. P. Multiannual simulations with a 3D chemical transport model. *J. Geophys. Res.* **104,** 1781–1805 (1999).
20. Swinbank, R. & O'Neill, A. A stratosphere-troposphere data assimilation system. *Mon. Weath. Rev.* **122,** 686–702 (1994).
21. Lefèvre, F., Figarol, F., Carslaw, K. S. & Peter, T. The 1997 Arctic ozone depletion quantified from three-dimensional model simulations. *Geophys. Res. Lett.* **25,** 2425–2428 (1998).
22. Becker, G., Müller, R., McKenna, D. S., Rex, M. & Carslaw, K. S. Ozone loss rates in the Arctic stratosphere in the winter 1991/1992: Model calculations compared with Match results. *Geophys. Res. Lett.* **25,** 4325–4329 (1998).
23. World Meteorological Organization *Scientific Assessment of Ozone Depletion: 1994* (Rep. No. 7, Global Ozone Research and Monitoring Project, Geneva, 1995).
24. Shindell, D. T., Rind, D. & Lonergan, P. Increased polar stratospheric ozone losses and delayed eventual recovery owing to increasing greenhouse-gas concentrations. *Nature* **392,** 589–592 (1998).

Acknowledgements. We thank P. Newman for information about the 1998 TOMS data, H. Teyssèdre for TOMS calculations, and J. A. Pyle for help and support. This work was supported by the UK Natural Environment Research Council.

Correspondence and requests for materials should be addressed to M.P.C. (e-mail: martyn@lec.leeds.ac.uk).

2-Methylhopanoids as biomarkers for cyanobacterial oxygenic photosynthesis

Roger E. Summons*, Linda L. Jahnke, Janet M. Hope* & Graham A. Logan*

* *Australian Geological Survey Organisation, GPO Box 378, Canberra, ACT 2601, Australia*

† *Exobiology Biology Branch, NASA Ames Research Center, Moffett Field, California 94035, USA*

Oxygenic photosynthesis is widely accepted as the most important bioenergetic process happening in Earth's surface environment[1]. It is thought to have evolved within the cyanobacterial lineage, but it has been difficult to determine when it began. Evidence based on the occurrence and appearance of stromatolites[2] and microfossils[3] indicates that phototrophy occurred as long ago as 3,465 Myr although no definite physiological inferences can be made from these objects. Carbon isotopes and other geological phenomena[4,5] provide clues but are also equivocal. Biomarkers are potentially useful because the three domains of extant life—Bacteria, Archaea and Eukarya—have signature membrane lipids with recalcitrant carbon skeletons. These lipids turn into hydrocarbons in sediments and can be found wherever the record is sufficiently well preserved. Here we show that 2-methylbacteriohopanepolyols occur in a high proportion of cultured cyanobacteria and cyanobacterial mats. Their 2-methylhopane hydrocarbon derivatives are abundant in organic-rich sediments as old as 2,500 Myr. These biomarkers may help constrain the age of the oldest cyanobacteria and the advent of oxygenic photosynthesis. They could also be used to quantify the ecological importance of cyanobacteria through geological time.

In the Bacteria, bacteriohopanepolyols (BHP) are amphiphilic membrane biochemicals[6] that serve a regulating and rigidifying function similar to that of sterols in the Eukarya. The hydrocarbon skeletons of BHP are extremely refractory and resist biodegradation to become incorporated into kerogen or bound into sulphur-linked macromolecules. They also survive high geothermal gradients accompanying hydrocarbon generation and ultimately appear in petroleum as defunctionalized and stereochemically modified[7] 'geohopanes'. Although many aspects of the preservation of BHP are well understood, there remains uncertainty about the sources of BHP and environmental controls on their abundance and distribution. This study assesses the role of cyanobacteria as a source of fossil hopanoids.

Table 1 summarizes the hopanoid contents of cultured cyanobacteria and mat communities that we analysed, along with data extracted from the literature. The high polarity and complexity of the hydrophilic side chains of BHP[8] precludes a generalized gas chromatography–mass spectrometry (GC–MS) analysis that detects all hopanoids. Accordingly, we applied the methodology of ref. 9 (Fig. 1) in our survey of the occurrence of hopane skeletons in cultures and environmental samples. Structural variation in the hydrophobic pentacyclic triterpane skeleton of BHP appears to be very limited. Unsaturation (Δ6 and/or Δ11) is rare, but supplementary methyl substituents at the 2α, 2β and 3β positions of ring-A have been reported often and may indicate metabolism in some bacteria. Methylation at C3 has been reported for a variety of methanotrophic, methylotrophic and acetic bacteria[9,10]. Methylation at C2 is common in cyanobacteria[9,11], as shown in Table 1, although it is not exclusive to this group. Of those other bacteria that have been studied, 2-methylhopanoids have also been found in pink pigmented faculative methylotrophs (PPFMs) related to *Methylobacterium organophilum*[12] and some nitrogen-fixing bacteria